The PHARAO Space Clock: Results on the Ground Operation of the Engineering Model.

(Invited Paper)

Philippe Laurent, Chistian Jentsch
André Clairon, Pierre Lemonde
Giorgio Santarelli
Observatoire de Paris, SYRTE
61, av. de L'Observatoire
75014 Paris, France
Email: philippe.laurentl@obspm.fr

Michel Abgrall, Christian Sirmain
Frederic Picard, Christophe Delaroche
Olivier Grosjean, Didier Blonde
Michel Chaubet, Philippe Guillemot
Jean François Vega, Isabelle Zenone
Nadine Ladiette
Centre National d'Etudes Spatiales
18 avenue Edouard Belin
31401 Toulouse, France

Christophe Salomon
Laboratoire Kastler Brossel
24 rue Lhomond
75231 Paris, France

***Abstract*— We present the first results of the engineering model of the cold atom space clock PHARAO. A relative frequency stability of $4.2 \times 10^{-13} t^{-1/2}$ with a quartz oscillator and of $2.5 \times 10^{-13} t^{-1/2}$ with a cryogenic oscillator have been obtained on the ground with a single path in a Ramsey cavity designed for microgravity operation.**

I. Introduction

The cold atom space clock PHARAO (Projet d'Horloge Atomique à Refroidissement d'Atomes en Orbite) is a key element of the European space mission ACES (Atomic Clock Ensemble in Space [1]). The ACES mission, managed by the European Space Agency, has three main objectives. The first one deals with the operation and study of the laser cooled cesium clock to reach a frequency accuracy of 10^{-16} in space. The second one is to perform fundamental metrology by comparing the clock signal with ground based clocks via a two way time transfer link. The third one is to perform fundamental physics tests such as a new measurement of the red shift at 2 parts per million and a contribution to a search for variations of fundamental physical constants. The expected time transfer resolution is 0.2 ps at 300 seconds and 6 ps from 1 to 10 days. A H-maser developed by the Observatoire Cantonal de Neuchâtel is the second ACES clock and will be used as a stable frequency reference for mid term duration.

The French space agency CNES is the prime contractor of the PHARAO clock. The development plan includes the construction of 3 devices: an engineering model (EM) fully operational is used to test the clock design and verify the performances. It allows identifying possible problems and finding the solutions for the flight model (FM), the third and last system to be constructed. The second device is a structural and thermal model (STM) used to test the thermal and mechanical environments required for the space qualifications. This model is not operational but fully representative in term of structure, materials, mass, thermal conductivity and power dissipation. The EM has been delivered to CNES on 2006 and the STM has undergone the tests.

In the following we present the EM clock. The first part is devoted to the clock description and the second one gives the first results of the whole clock.

II. Clock architecture

The Figure 1 shows the scheme of the clock. It includes four sub-systems which have been separately developed by some manufacturers. The cesium tube is the place where the cesium atoms are cooled, prepared, interrogated by the microwave frequency and detected. It received from the laser source 10 laser beams through optical fibers: 6 for the cooling process, 2 for the preparation and 2 for the detection. It sends to the laser source some photodiode signals in order to stabilize the laser power for the different phases of the atom manipulation. These systems have been developed by EADS-SODERN. The microwave source developed by TAS, based on a 5 MHz ultra-stable quartz oscillator from CMAC, feeds the 9.2 GHz signal to the preparation and interrogation microwave cavities of the cesium tube. It sends a 100 MHz signal to the ACES comparator for phase comparisons with the H-maser. For tests or quartz oscillator failure it receives an external 100 MHz to synthesize the microwave signals. Finally a computer (developed by EREMS) with a dedicated software (developed by CSSI) manages and monitors the clock operation. It is also the communication link with the ACES payload.

A. Cesium tube

The scheme of the cesium tube is shown in figure 2. The main structure is made up of an $80cm$ long vacuum chamber maintained by two supports screwed on the base plate. The chamber structure has 7 parts in titanium linked together by

1-4244-0647-1/07/$20.00 ©2007 IEEE

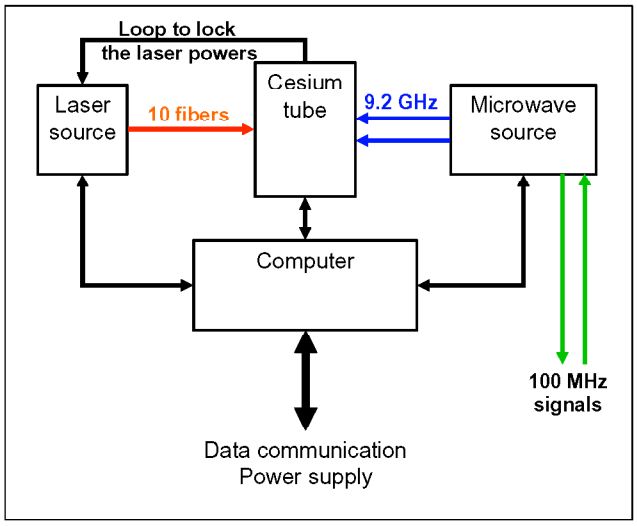

Fig. 1. Diagram of the PHARAO clock architecture. The black, red, blue and green lines represent respectively the electrical, optical and radiofrequency connections.

aluminum gasket. One side is closed by a cesium reservoir filled with $3g$ of cesium to ensure at least ten years of lifetime. The liquid cesium is trapped by capillarity inside thick titanium foam covering the inner surfaces. A motorized valve opens the reservoir toward the atomic capture zone. The cesium flux is regulated by the valve aperture and by the reservoir temperature (between 40 and 60°C). In the capture zone we have measured a cesium pressure which can be adjusted between 10^{-8} Pa to 10^{-5} Pa to optimize the dynamic of the molasses loading.

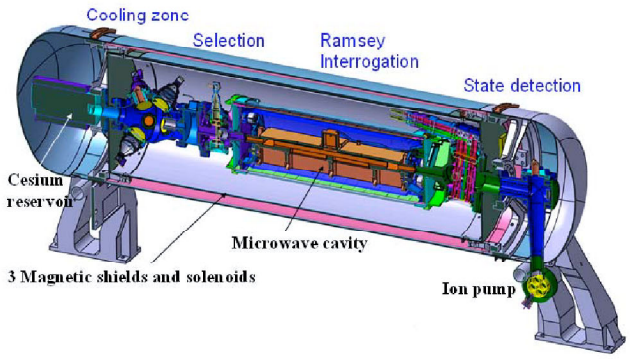

Fig. 2. Cross section of the PHARAO clock tube. Atoms from a cesium vapor are captured in the cooling zone. After launch and selection into a well-defined magnetic substate, atoms interact with a microwave field in the two active sections of a Ramsey cavity. Atoms in both hyperfine levels are detected downstream by laser induced fluorescence. The overall length of the device is 990mm and the mass is 45kg. (Courtesy EADS SODERN)

The 6 capture beams have a waist of $5.5mm$ and a total size of $26mm$. The polarization configuration is lin perp. lin. Each beam collimator has a polarizing beam splitter to reflect the counter propagating beam toward a photodiode used to lock the laser power. A seventh photodiode collects the cesium fluorescence during the molasses loading. The cold atom cloud is launched along the $[1, 1, 1]$ direction related to the frame defined by the laser beams. After launching all the atoms are in the $F = 4$ hyperfine level before to enter in a cylindrical TE_{001} microwave preparation cavity with $25mm$ and $40mm$ cut-off waveguides. This cavity induces a selective transition between the same Zeeman sub-level of the two hyperfine levels $F = 4 \rightarrow F = 3$ ($m = 0$ for clock operation or $m = 1$ for magnetic field evaluation).

At the cavity output a first laser beam can pump the atom in the $F = 4$ level. It is followed by a second laser beam tuned to the D_2 line cycling transition $(F = 4, F = 5)$ to push away the atoms in $F = 4$ hyperfine level. By pulsing the first beam, the $F = 3$ atom cloud can be sliced to study the atomic distribution. The remaining $F = 3$ atoms enter in the interrogation zone which bears a Ramsey copper cavity of $20cm$ long with $30mm$ cut-off waveguides. A magnetic shield with a solenoid and 2 compensation coils at both ends surround the interrogation zone. They define the clock bias magnetic field and its homogeneity.

The performances of the cavity flight model have been verified inside the LNE-SYRTE fountain FO1 [2]. No frequency shift (phase distribution, magnetic anomaly and microwave leakage) appears at the experimental resolution level of 4×10^{-16}. As the cavity induced phase shift is proportional to the atomic velocity we will re-evaluate this effect in microgravity thanks to the new physical variable: the atomic velocity which can be changed over two orders of magnitude.

In this interrogation zone the vacuum level is ensured by 5 getters with a pumping rate of 2l/s. Besides graphite getters prevent cesium migration from the capture region.

Finally, the cold atom cloud enters the detection zone. It successively passes through 4 laser beams tilted by 8° with respect to the atom velocity. The first and fourth are standing waves with circular polarization tuned to the cesium D_2 line $(F = 4, F = 5)$ cycling transition. They induce fluorescence signals which are collected by two condensers with an efficiency of 5%. The two photodiode signals are digitized by the computer to calculate the transition probability. The second beam tuned to the $(F = 4, F = 5)$ transition is a traveling wave to push away atoms in the $F = 4$ level after their detection. The third beam tuned to the $(F = 3, F = 4)$ transition pumps the $F = 3$ atoms to the $F = 4$ level. These atoms are subsequently detected by the fourth standing wave laser beam. As the beams are tilted, the residual thermal cesium beam which escapes from the capture zone is off resonance by $40MHz$. The stray fluorescence emitted by this fast beam is then reduced by at least a factor of 10 and it reaches the same very low level as the residual stray light [3]. Their contributions to the detected atomic signal are then negligible in usual operation. The photo detection has a transfer gain of 15 V for 1 μW radiated by the atoms and the noise level is $4\mu V/\sqrt{Hz}$ in the $1 - 100Hz$ frequency band.

Finally the vacuum chamber closes with a 2l ion pump. The vacuum level deduced from the calibrated ion pump current is

2×10^{-7} Pa and decreased to 10^{-8} Pa when the cesium tube is under vacuum (as in the space).

A second magnetic shield encloses the vacuum chamber from the capture zone to the detection. Two inner coils define the magnetic field in the preparation cavity and the detection. Compensation coils are also positioned close to the first magnetic shield apertures to improve the magnetic homogeneity. A coil wound around the second shield and a magnetic probe allow an active compensation of the external magnetic field fluctuations. Finally a third magnetic shield encloses the whole device. The passive magnetic attenuation reaches 20000 inside the interrogation zone and is multiply by 17 when the active compensation is in operation.

Two wires along the tube axis pass through the magnetic shields. The first one is used to demagnetize the shields. The maximum injected current is 2 A at a frequency of 0.1 Hz. The second one is used to induce magnetic transitions $\Delta m = 1$ inside one hyperfine level of the cesium atoms. The transition probability reaches a maximum when the injected oscillating current is at resonance. By pulsing the current at different atomic locations we can then measure the local magnetic field. Obviously a hyperfine transition is performed in the second zone of the Ramsey cavity to detect the resonance signal.

The temperature regulation of the interrogation zone is ensured by two heaters and the temperature is measured by 2 calibrated platinum probes to determine the blackbody frequency shift.

All the laser beams are provided by the laser source through maintaining polarizing optical fibers.

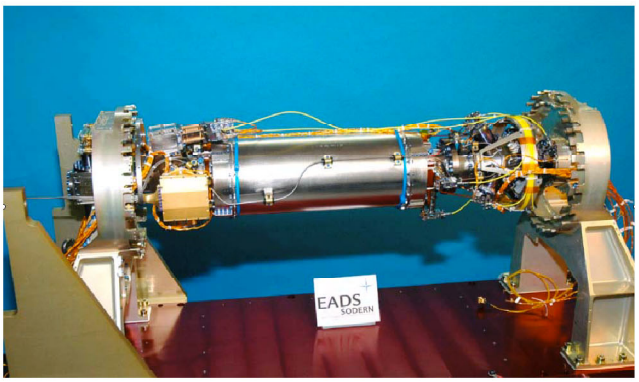

Fig. 3. Picture of the cesium tube. The two external magnetic shields are removed.

B. Laser source

The laser source architecture is shown in figure 4. An extended cavity diode laser (ECDL) is locked to the saturated absorption crossover resonance of cesium ($6S_{1/2}, F = 4 \rightarrow 6P_{3/2}, F = 4/5$) through an acousto-optic modulator (AOM1). The ECDL design has an intra-cavity etalon for rugged and reliable behavior [4] [5]. The laser beam passes through a $30dB$ optical isolator. Its power is $30mW$ for a diode laser current of $70mA$. $5mW$ are used to perform the frequency locking. The diode laser current is modulated at $500kHz$ and the absorption signal is synchronously demodulated to provide the error signal. This signal is applied to the diode laser current and to the PZT transducer which drives the cavity length of the ECDL. The measured frequency noise level reaches $10^4 Hz^2/Hz$ at a Fourier frequency of $100Hz$. By changing the AOM1 RF frequency the laser frequency can be tuned over $80MHz$ with a rate of $260kHz/\mu s$. This ECDL/AOM1 combination provides the frequency reference for each atom process: capture, cooling, selection and detection.

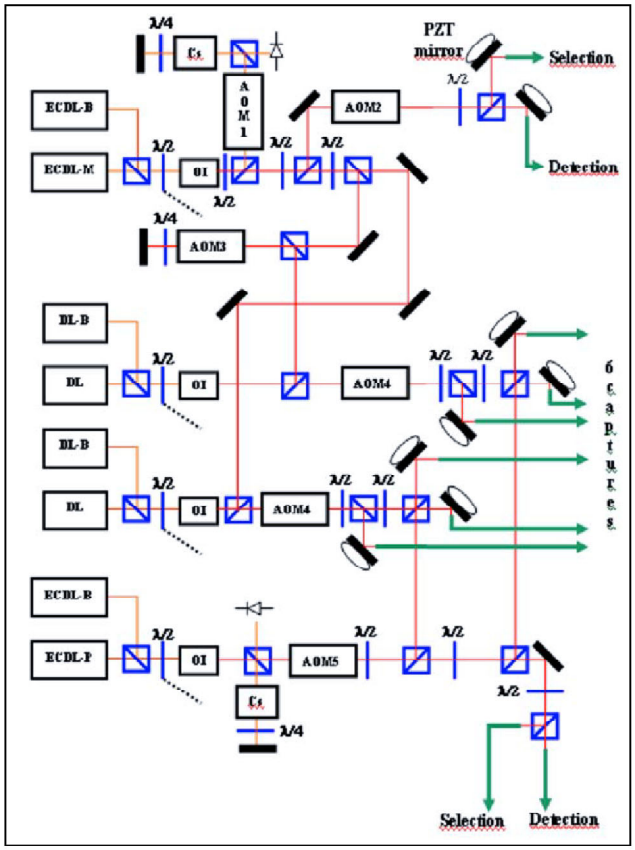

Fig. 4. Optical architecture of the laser source. The 5 mechanical shutters are not represented. The optical fibers are indicated by the green outgoing arrows. ECDL: extended cavity diode laser (M:master, P: pump, B: backup). DL: diode laser. AOM: acousto-optic modulator. OI: optical isolator. Cs: cesium cell.

As the AOM1 is in the frequency loop, the 25 mW laser beam alignment is not perturbed by the frequency tuning. The beam is then split into three beams. One beam is coupled into two optical fibers through an acousto-optic modulator (AOM2). It is used for the atomic detection (10 mW) and selection (5mW). The laser power is adjusted and controlled by the AOM2 RF power. The resolution is 10 μW with a dynamic range of about 25 dB. This AOM2 operates at a frequency of 75 MHz. The second part of the beam double passes through a third acousto-optic modulator (AOM3) before injecting a slave diode laser. The AOM3 frequency can be

adjusted from 90 MHz to 86 MHz to launch atoms (from 5 cm/s to 5 m/s) with the moving molasses method [6]. The third beam injection-locks a second slave diode laser. The slave diode lasers are injected over a 2 mA current variation. A photodiode behind a cesium cell is used to check the injection. After an optical isolator, the slave laser beam passes through a 90 MHz acousto-optic modulator (AOM4) and is divided in three beams. The two slave lasers provide the 6 beams (3+3 counter propagating) to make the optical molasses geometry. The AOM4 RF power determines the capture and cooling intensities which can be decreased with a slew rate of 40dB over 300μs to perform adiabatic cooling after the atom launching. Each beam is reflected by a mirror mounted on 4 PZT transducers. This allows a fine alignment (θ, φ) of the beam on the fiber core and a power balancing in each of the three molasses beam pairs at 1% level. The slave diode laser current is 110 mA and the fiber output power is 12 mW.

A second ECDL is locked to the cesium crossover resonance $(6S_{1/2}, F = 3 \rightarrow 6P_{3/2}, F = 3/4)$. The beam passes through a 101 MHz and is split into four. Two beams are injected into optical fibers to repump the atoms during selection and detection. The two others are superimposed on the slave beams.

All fixed frequency AOMs have an optical efficiency better than 80 % with a RF power of 150 mW. They are also used as actuators for the laser power servo-loop and can switch off the laser beam intensity by 60 dB. In addition 5 mechanical shutters ensure complete extinction of the beams (120 dB).

Both ECDLs and slave lasers have a back-up in case of diode failure. The integrated laser source is shown in figure 5. The optical components are mounted on a double sided optical bench. The bench is fixed on the baseplate through 4 dampers. The temperature regulation of the bench is ensured by a combination of heaters and Peltier coolers to maintain the temperature at 26°C when the baseplate temperature varies from 10 to 35°C. All the electronics package is under the bench.

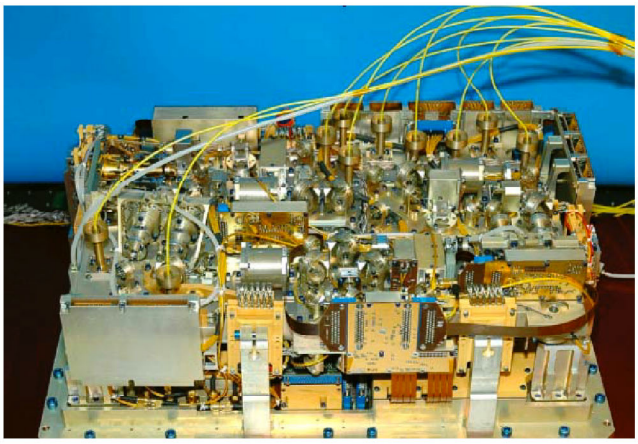

Fig. 5. Picture of the integrated laser source with cover removed. The dimensions are $530 \times 350 \times 150$ mm^3 and the mass is 20.054 kg. The ten polarization maintaining optical fibers in yellow guide the laser beams to the cesium tube. All diode lasers (JDSU) are mounted on a Peltier cooler for temperature regulation within 2 mK. (Courtesy EADS SODERN).

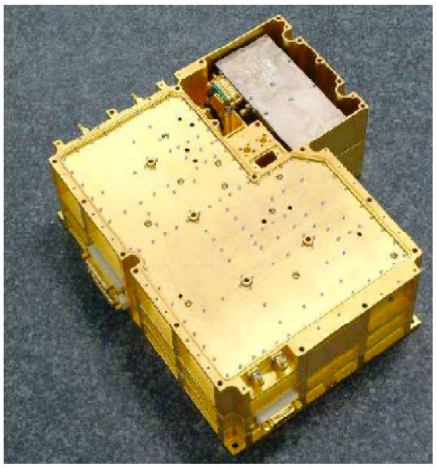

Fig. 6. A picture of the microwave source. On the upper right side we can see the quartz oscillator. The total mass is 7 kg, the power dissipation is 21 W, and the dimensions are $300 \times 270 \times 177 mm^3$. (Courtesy THALES)

C. Microwave source

The microwave source feeds the two cavities of the cesium tube (see fig. 6). The microwave generation is based on the frequency multiplication of a very low phase noise quartz oscillator up to 9.192 GHz. The quartz oscillator frequency stability has been measured against a sapphire cryogenic oscillator [8] at a level of 6×10^{-14} for time durations below 10 seconds. The 5 MHz quartz frequency is multiplied and mixed with the signal of a Direct Digital Synthesizer (DDS) to supply a 100 MHz signal. The DDS is mainly used to frequency lock (response time $>$ 2s) the 100 MHz signal to an external oscillator (the H-maser of the ACES system). The purpose of this loop is to optimize at all Fourier frequencies the frequency noise spectrum of the 100 MHz signal.

The 100 MHz signal is multiplied and mixed with the signal of a second DDS which drives the microwave frequency at 9.192 GHz. Two microwave signals are generated with independent amplitude and frequency: one for the atomic preparation and the second for the interrogation. As the frequency is defined by the same DDS, an external digital signal (PCP) switches between two DDS registers to quickly commute the frequency after the atoms leave the preparation cavity. This signal also switches off the preparation cavity microwave signal by 80 dB to ensure insignificant microwave leakage.

The 9.2 GHz noise level is mainly determined by the quartz oscillator phase noise; the contribution of the other elements is 10 dB lower. The microwave source has been extensively tested using the LNE-SYRTE FO2 atomic fountain. Using a cryogenic oscillator as interrogation oscillator and sufficient atom number, this fountain displays a frequency stability of $1.6 \times 10^{-14}\ \tau^{-1/2}$ [7]. With the PHARAO synthesis chain, weakly phase locked on the 100 MHz signal synthesized from the cryogenic oscillator signal, the frequency stability is 7 $\times$

$10^{-14}\,\tau^{-1/2}$[3]. It is the best frequency stability ever achieved in a fountain with a quartz oscillator as interrogation oscillator.

D. Computer and software

The computer communicates with the sub-systems by 3 different RS422 lines. It sends and reads numerical values of the physical parameters. In addition, the computer triggers the clock cycle events through 23 lines to change for instance AOM frequencies, mechanical shutter states or the microwave source frequency. The computer also digitizes analog signals. The main signals are the fluorescence signal in the capture zone as well as the detection fluorescence signals to measure the clock transition probability. Finally, the computer is connected to the ACES payload through a RS422 line for telemetry and telecommand.

The computer manages the clock through background processes and through routines. The background processes concern all the very low frequency servo-loops as temperature regulations or the 100 MHz frequency loop, the monitoring of the physical parameters and the ACES communications. The routines concern the cycle operations of the clock by sending the trigger pulses, receiving and processing the clock data (fluorescence signals, laser power,...).

III. Experimental results

The laser source, the cesium tube and the microwave source have been assembled in the clean room at CNES, Toulouse (see fig. 7). Obviously the clock only works when the cesium tube is vertical. During these preliminary experiments the laser source has been working under air. The optical connection with the cesium tube is then made through long optical fiber savers. Consequently the optical losses are higher and the laser power in the capture zone is only 6 mW per beam instead of 12 mW.

A. Cold atoms

In the first configuration the capture zone is at the bottom and the atoms are launched upwards at a velocity of $3.4m/s$ in order to reach the detection zone. The molasses loading is as expected and time of flight signals with excellent signal to noise ratio are obtained (see figure 8), indicating extremely low levels of stray light in the detection region and very good laser intensity and frequency stability. By integrating the time of flight signal over time we have deduced a number of detected atoms of 10^7 in accordance with the expectation from laser power and detuning in the cooling zone (about 20% of the captured atoms are detected).

As the apogee of the cloud is 5 cm higher than the detection beams we have been able to detect the cloud when it returns back to the detection in order to measure the velocity distribution. The figure 9 shows the longitudinal shapes of the cloud when it is detected on the way up or in the way down. The time difference between the two signals is 150ms. A significative widenening only appears in the wings of the cloud. The atoms in the right side of the cloud have left the capture beams before the cooling process ends. Consequently their velocity distribution is higher.

Fig. 7. The PHARAO space clock under test in CNES, Toulouse. On Earth the tube is set vertical. The microwave source is hidden by the tube. The laser source (on the left) is covered with multilayer insulator. On this picture the chamber in which the vacuum tests are performed is opened. The clock can be operated at atmospheric pressure or in vacuum.

We have also tested the launched direction of the atoms. To perform this experiment the cesium tube is turned to have the capture zone at the top. Its verticality is aligned by maximizing the detection signal when the atoms fall down without initial velocity. The atoms are then launched with a velocity of 3.41m/s and the detection signal is recorded for some different cesium tube orientations. The maximum number of atoms is obtained when the cesium tube is vertical with a resolution better than 1 mrd. That is the proof the launching direction is well aligned to the Ramsey cavity axis. Consequently no interrogation asymmetry is introduced. An asymmetry could induce additional clock frequency shift.

B. Clock operation

When the microwave preparation signal is turned on the atomic selection efficiency in one Zeeman sub-level is better than 99.9% and we detect up to 10^6 atoms (the magnetic C-field is 0.2μT). Figure 10 shows the measured transition probability when the interrogation microwave frequency is scanned near 9 192 631 770 Hz. The capture zone is at the bottom and the atom velocity is 3.41 m/s. The resulting interrogation time is 90 ms and leads to a central fringe width of 5.5 Hz. The signal to noise ratio is better than 500. As expected, the central fringe contrast is not 100% since the Ramsey interrogation is not symmetrical (the rabi frequency is not the same inside the two interaction zones) due to the atoms deceleration induced by the gravity.

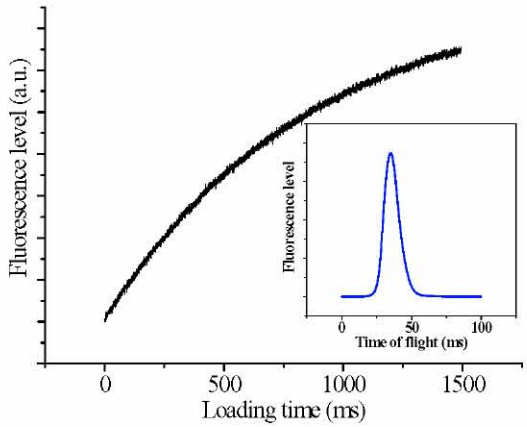

Fig. 8. The fluorescence signal evolution during the atom capture. The time constant is 800 ms and the cesium pressure is 9×10^{-6} Pa. The inset is the detected time of flight signal when the atoms are launched upward at a velocity of 3.4 m/s.

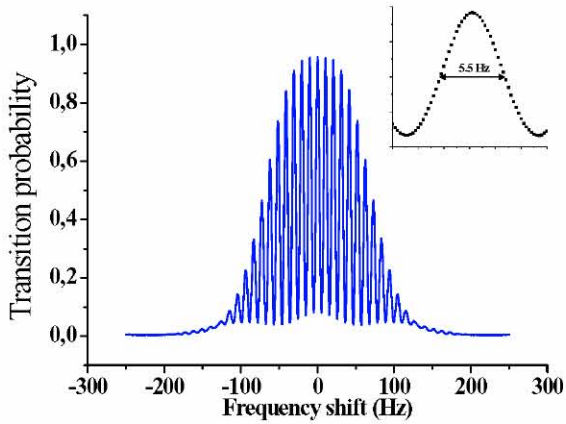

Fig. 10. Experimental Ramsey fringes. The upwards launch velocity is 3.4 m/s and the width of the central resonance is 5.5 Hz (insert).

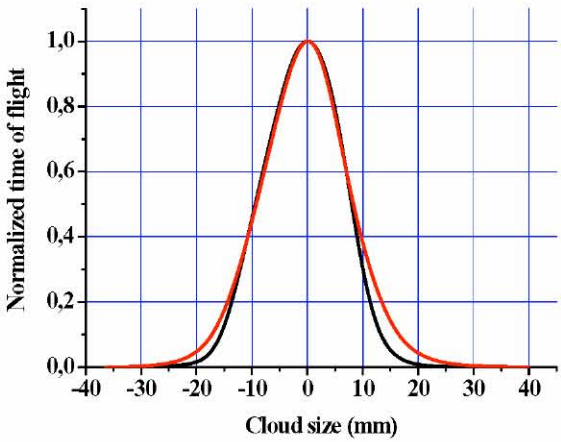

Fig. 9. The longitudinal shape of the cloud measured upwards (black line) and downwards (redline). The signals have been normalized and filtered.

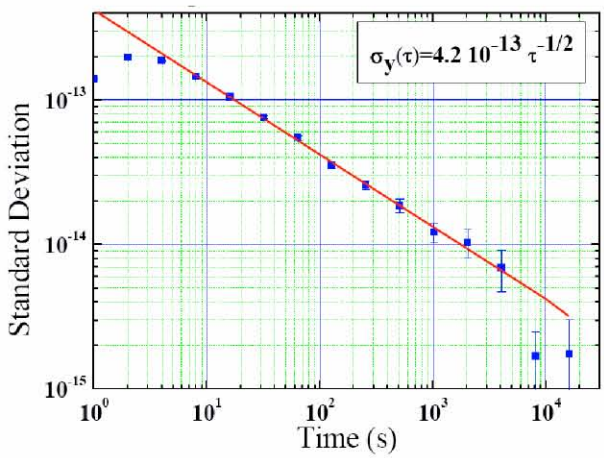

Fig. 11. Frequency stability of the clock measured against a H-maser.

When the microwave frequency is locked on the central fringe the frequency stability measured against a cryogenic saphir oscillator phase locked on a H-maser is $4.2 \times 10^{-13}t^{-1/2}$ (see fig. 11). The clock cycle is 400 ms of loading time, 200 ms of free flight and 80 ms of detection. The stability is mainly defined by the projection noise [9] (inversely proportional to the square root of the number of detected atoms) and the aliasing phenomena of the microwave phase noise generated by the quartz oscillator [10] [11].

To make this phase noise contribution negligible, the 100 MHz external signal of the microwave source is fed by the cryogenic oscillator. The frequency stability is then improved and reaches $2.3 \times 10^{-13}t^{-1/2}$ (see fig.12). This value is in agreement with the expected projection noise. The quartz phase noise has consequently a contribution of $3.5 \times 10^{-13}t^{-1/2}$ to the clock frequency stability with an atomic resonance as large as 5.5 Hz. By using the measured spectral density phase noise of the quartz oscillator and simulating the clock operation we find the same degradation of the frequency stability.

IV. Conclusion

The first PHARAO science run described in this paper has demonstrated the essential operations of a cold atom cesium clock designed for microgravity environment. The next step involve the clock assembling on the same baseplate and the tests of the flight software. It will be followed by the evaluation of the frequency accuracy. With a frequency stability of $2-4 \times 10^{-13}t^{-1/2}$, we willl easily obtain a frequency accuracy resolution of 10^{-15}. These measurements will be performed in thermal-vacuum environment to be representative of the environment experienced by the PHARAO instrument

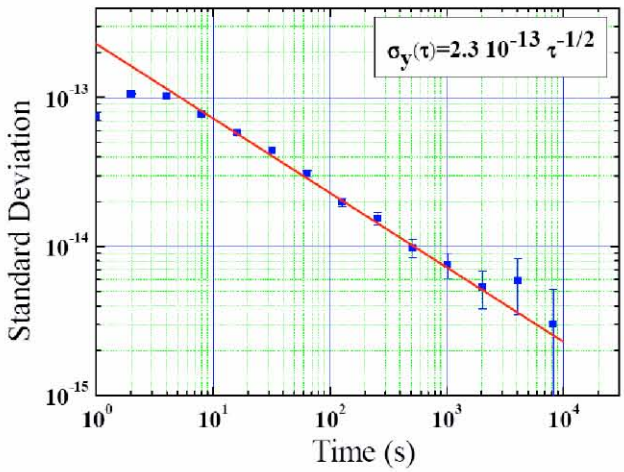

Fig. 12. Frequency stability of the clock when the 100 MHz signal of a cryogenic oscillator replaces the quartz oscillator one.

on board the international space station. The goal of these performance evaluations is to safely anticipate an accuracy of 10^{-16} in space.

V. Acknowledgements

The authors would like to acknowledge the industrial teams from EADS-SODERN, THALES, CMAC, EREMS, CSSI which provided the various PHARAO sub-systems. We thank the members of the CNES technical support, Michel Aubourg from IRCOM for the simulations of the microwave cavity field, Sylvie Léon and Richard Bonneville for continuous support. We acknowledge the ACES science team for numerous stimulating discussions.

This work is supported by CNES, CNRS, LNE, Observatoire de Paris and région Ile de France (IFRAF). The SYRTE is a unit associated to CNRS UMR 8630. The Laboratoire Kastler Brossel is a unit associated to CNRS UMR 8552 and to University Pierre and Marie Curie.

References

[1] C. Salomon, et al., Cold atoms in space and atomic clocks: ACES, C. R. Acad. Sci. Paris, Ser. IV 2 (2001) 1313.

[2] C. Vian, P. Rosenbush, H. Marion, S. Bize, L. Cacciapuoti, S. Zhang, M. Abgrall, D. Chambon, I. Maksimovic, P. Laurent, G. Santarelli, A. Clairon, A. Luiten, M. Tobar, C. Salomon, BNM-SYRTE fountains : recent results, IEEE T. Instrum. Meas. 44 (2004).

[3] Laurent, P.; Abgrall, M.; Jentsch, C.; Lemonde, P.; Santarelli, G.; Clairon, A.; Maksimovic, I.; Bize, S.; Salomon, C.; Blonde, D.; Vega, J.; Grosjean, O.; Picard, F.; Saccoccio, M.; Chaubet, M.; Ladiette, N.; Guillet, L.; Zenone, I.; Delaroche, C. & Sirmain, C. (2006), 'Design of the cold atom PHARAO space clock and initial test results', Applied Physics B: Lasers and Optics V84(4), 683–690.

[4] F. Allard et al., automatic system to control the operation of an extended cavity diode laserRev. Sci. Instrum. 75 (2004) 54.

[5] X. Baillard, A. Gauguet, S. Bize, P. Lemonde, Ph. Laurent, A. Clairon, P. Rosenbusch, Interference-filter-stabilized external-cavity diode lasers, Optics Communications, 266 (2006) 609–613

[6] A. Clairon, et al., A cesium fountain frequency standard: recent results, IEEE T. Instrum. Meas. 44 (1995) 128.

[7] S. Bize, et al., Advances in atomic fountains, C. R. Physique 5 (2004) 829–843.

[8] A.G. Mann, S. Chang, A.N. Luiten, Cryogenic sapphire oscillator with exceptionally high frequency stability, IEEE T. Instrum. Meas. 50, (2001) 519.

[9] G. Santarelli, Ph. Laurent, P. Lemonde, A. Clairon, A.G. Mann, S. Chang, A.N. Luiten, C. Salomon, Quantum Projection Noise in an Atomic Fountain: A High Stability Cesium Frequency Standard, Phys. Rev. Lett., 82 (1999), 4619.

[10] G. Dick, in Proceedings of the Precise Time and Time Interval Meeting, Redondo Beach, 1987 (U.S. NavalObservatory, Washington, DC, 1988), 133–147.

[11] A. Santarelli, C. Audoin, A. Makdissi, P. Laurent, G.J. Dick, A. Clairon, Frequency stability degradation of an oscillator slaved to a periodically interrogated atomic resonator, IEEE Ultrasonics, Ferroelectrics and Frequency Control, 45 (4),1998, 887 - 894.